Journal of Power and Energy Engineering, 2026, 14(11), 68-81
https://www.scirp.org/journal/jpee
ISSN Online: 2327-5901
ISSN Print: 2327-588X

Optimizing Ag-Doped TiO_2 Coatings for Enhanced Visible-Light Photocatalythic on Glazed Ceramic Tiles

Zulkifli Mohd. Rosli[1], Nurhafizah Zaharuddin[2], Jariah Mohamad Juoi[2], Thangaraj Joseph Sahaya Anand[3]

[1]School of Technical Foundation and Diploma Studies, Universiti Teknikal Malaysia, Melaka, Malaysia
[2]Faculty of Industrial and Manufacturing Technology and Engineering, Universiti Teknikal Malaysia Melaka, Melaka, Malaysia
[3]School of Computing, MIT Vishwaprayag University, Solapur, India
Email: zmr@utem.edu.my

How to cite this paper: Rosli, Z.M., Zaharuddin, N., Juoi, J.M. and Anand, T.J.S. (2026) Optimizing Ag-Doped TiO_2 Coatings for Enhanced Visible-Light Photocatalythic on Glazed Ceramic Tiles. *Journal of Power and Energy Engineering*, **14**, 68-81.
https://doi.org/10.4236/jpee.2026.1411005

Received: October 9, 2026
Accepted: November 10, 2026
Published: November 13, 2026

Copyright © 2026 by author(s) and Scientific Research Publishing Inc.
This work is licensed under the Creative Commons Attribution-NonCommercial International License (CC BY-NC 4.0).
http://creativecommons.org/licenses/by-nc/4.0/
Open Access

Abstract

Titanium dioxide (TiO_2) coatings are widely studied for self-cleaning ceramic applications due to their strong photocatalytic activity under ultraviolet (UV) light. However, their effectiveness under visible light is limited by a wide bandgap and rapid electron-hole recombination. This study addresses this limitation by investigating silver (Ag) doping as a strategy to enhance the visible-light photocatalytic response of TiO_2 coatings. Ag-TiO_2 coatings with varying Ag contents (2.5, 5, and 7.5 mol%) were deposited on glazed ceramic tiles via a dip-coating method, followed by calcination at 500˚C. The structural, morphological, and compositional characteristics of the coatings were examined using X-ray diffraction (XRD), scanning electron microscopy (SEM), field emission SEM (FESEM), and energy-dispersive X-ray spectroscopy (EDX). Photocatalytic performance was assessed by monitoring the degradation of methylene blue (MB) under both UV and visible light. The results indicate that the 5 mol% Ag formulation yielded the highest observed photocatalytic activity under the reported visible-light conditions. The anatase crystallite size increased from 8.46 nm at 0 mol% Ag to 14.5 nm at 5 mol% Ag; therefore, the activity maximum cannot be attributed to reduced crystallite size. Coating thickness and the observed morphological defects should also be considered when interpreting this result. The findings underscore the potential of Ag-doped TiO_2 coatings as effective, visible-light-active materials for self-cleaning ceramic surfaces, with broader implications for antibacterial and environmental remediation applications.

Keywords

Ag-Doped TiO_2, Visible-Light, Photocatalysis, Glazed Ceramic Tile

1. Introduction

Ceramic tiles are widely used in residential, commercial, and public spaces due to their durability, aesthetic appeal, and ease of maintenance. However, these surfaces are particularly common in moisture-prone environments such as bathrooms, kitchens, and hospitals. Therefore, these surfaces are susceptible to microbial contamination, which can pose serious health risks. While glazed ceramic tiles are less porous and easier to clean than unglazed variants, they are still prone to bacterial colonization, especially under conditions that promote microbial growth [1]. To address surface contamination, nanocoating technologies have gained attention for their ability to confer self-cleaning and antimicrobial properties. Although extensive research has been conducted on functional nanocoatings for metals, polymers, and textiles, their application on ceramic surfaces remains underexplored. Among the available technologies, photocatalytic coatings based on titanium dioxide (TiO_2) have emerged as promising candidates due to their chemical stability, environmental safety, and cost-effectiveness [2]-[6]. TiO_2 has demonstrated strong photocatalytic activity under ultraviolet (UV) irradiation, which can be harnessed for antimicrobial and pollutant degradation applications [3]. However, its wide band gap (3.0 - 3.2 eV) restricts its activation to the UV region ($\lambda < 380$ nm), which limits its functionality under visible light and natural sunlight [7]-[9]. To overcome this limitation, researchers have explored doping TiO_2 with noble metals such as silver (Ag). Ag doping can induce surface plasmon resonance effects, enhance visible-light absorption, and reduce the recombination rate of photogenerated charge carriers [10]-[14]. In addition to enhancing photocatalysis, Ag exhibits inherent antimicrobial properties, offering dual functionality even in the absence of light [15]. Previous studies have demonstrated that incorporating Ag into TiO_2 structures can significantly reduce the band gap and improve photocatalytic efficiency. For example, Onna *et al.* [16] successfully applied W-doped TiO_2 on ceramic tiles, while Ashraf *et al.* [17] and Abbad *et al.* [18] reported enhanced degradation rates and antimicrobial effects using Ag and graphene-based TiO_2 composites.

Despite these advancements, limited research has systematically examined the influence of varying Ag content on the structural and photocatalytic behavior of TiO_2 coatings applied to glazed ceramic tiles. The relationship between Ag loading, phase formation (e.g., Ag^0, AgO, Ag_2O), and photocatalytic efficiency, especially under visible light, remains inadequately understood. Furthermore, excessive Ag content may lead to agglomeration and reduced surface activity, indicating a need for optimization. Therefore, this study aims to investigate the effect of different Ag doping concentrations (2.5, 5, and 7.5 mol%) on the crystalline structure, microstructure, and photocatalytic performance of Ag-TiO_2 coatings deposited via dip-coating on glazed ceramic tiles. The coatings were heat-treated at 500˚C and characterized using XRD, SEM, FESEM-EDX, and evaluated for methylene blue degradation under both UV and visible light.

The findings from this study are expected to contribute valuable insights into the development of visible-light-active, self-cleaning ceramic surfaces. By optimizing Ag content, the results may facilitate the design of antimicrobial ceramic tiles suitable for hygienically sensitive environments such as healthcare facilities, food preparation areas, and public restrooms.

2. Materials and Methods

2.1. Preparation of Ag-TiO_2 Sol and Coating Deposition

An Ag-TiO_2 precursor sol was prepared using 4 mL titanium(IV) isopropoxide (TTIP, $Ti(OC_3H_7)_4$, 97%, Sigma-Aldrich) as the Ti source. A predetermined amount of TTIP was introduced into 64 mL of deionized water (Polyscientific) while the mixture was continuously stirred. Hydrochloric acid (0.4 mL, 37%, Merck) was subsequently introduced dropwise over 3 h to facilitate controlled hydrolysis of the titanium precursor and improve sol stability.

For silver incorporation, varying amounts of silver nitrate ($AgNO_3$, 99.9%, Merck) were dissolved in specific volumes of acetonitrile (CH_3CN, 99.5%, Merck) to yield solutions with nominal Ag contents of 2.5, 5.0, and 7.5 mol%. The mole percentage (mol%) was calculated using the molar ratio of silver ions (nAg^+) to the total moles in the binary mixture, defined as: Ag mol% = [n $AgNO_3$/n ($AgNO_3$ + nCH_3CN)] × 100. To prepare 50 mL of each solution, 4.092 g, 8.235 g, and 12.432 g of $AgNO_3$ were respectively transferred into 50 mL volumetric flasks and diluted to the mark with acetonitrile. Each prepared $AgNO_3$ solution was subsequently added dropwise into a TiO_2 sol under continuous magnetic stirring. Following complete incorporation, the resulting precursor mixtures were stirred for an additional 1 h to ensure homogeneity and subsequently aged at ambient temperature for 48 h prior to coating deposition.

Glazed ceramic tiles measuring 20 mm × 10 mm × 4 mm were selected as coating substrates. Surface preparation was carried out by ultrasonic cleaning in acetone, ethanol (95%, Polyscientific), and distilled water, with each cleaning step performed for 10 min. The substrates were subsequently dried at 110˚C for 2 h before undergo dip-coating procedure using mechanical dip coater (TEFINI Model DP1000).

During deposition, the ceramic substrates were withdrawn from the precursor sol at a constant rate of 30 mm min^{-1} following a 5 s dwelling period. After each deposition step, the coated substrates were allowed to dry in air for 3 h and then thermally dried at 110˚C for 30 min. The dip-coating and intermediate drying sequence was repeated for a total of five cycles, resulting in multilayer Ag-TiO_2 coatings with a relatively uniform surface coverage. The Ag-TiO_2 coatings deposited on glazed tiles were then heat-treated at 500°C with a heating rate of 2˚C/min.

2.2. Structural and Morphological Characterization

The surface morphology of the Ag-TiO_2 coatings was investigated using scanning

electron microscopy (SEM; JEOL JSM-6010PLUS/LV) and field-emission scanning electron microscopy (FESEM; HITACHI SU5000). In addition to morphological observation, the elemental composition and spatial distribution of the constituent elements within the coatings were examined by energy-dispersive X-ray spectroscopy (EDX) coupled with the FESEM system.

2.3. Photocatalytic Performance

The photocatalytic activity of the Ag-TiO_2-coated ceramic tiles was assessed by monitoring the degradation of methylene blue (MB, $C_{16}H_{18}N_3$, Merck) in accordance with ISO 10678:2010.

The coated substrates were tested under two irradiation conditions using a 40 W ultraviolet (UV) lamp and a 200 W visible-light lamp. Prior to testing, the coated tiles were irradiated with UV light for 24 h to eliminate residual surface organic contaminants. To establish adsorption-desorption equilibrium, the samples were immersed in 25 mL of an aqueous MB solution and maintained in the dark for 30 min. The initial MB concentration was 1×10^{-6} M, and the exposed coating area was 6.4×10^{-4} m^2. Photocatalytic evaluations were performed under a 200 W OSRAM visible-light lamp placed 16 cm above the dye solution. The lamp emission range was 600 - 700 nm. During exposure, the temperature inside the reaction chamber was maintained at approximately 25˚C using a cooling fan. After the dark-conditioning period, the samples were transferred to fresh 25 mL portions of the MB solution and exposed to visible radiation for 5 h. Aliquots of the dye were collected at 1 h intervals, and the changes in MB concentration derived from residual absorbance were monitored using a SHIMADZU UV-1700 UV-Vis spectrophotometer at 665 nm. A reference sample maintained under dark conditions was analyzed in parallel to account for non-photocatalytic dye removal. The percentage of MB degradation was computed using Equation (2).

The specific degradation rate (R) was calculated according to Equation (1):

$$R = \frac{\Delta A_\lambda \times v}{\Delta t \times \varepsilon \times d \times A} \tag{1}$$

where ΔA_λ is the absorption difference from one measurement to another (1 h to 5 h); v is the volume of MB solution used; Δt is the time difference; ε is the molar extinction coefficient of MB at 665 nm (ε = 7402.8 m^2/mol); d is the optical path length of the spectrophotometric cuvette, and A is the contact area between the MB solution and the photocatalyst.

The specific degradation rate (R) for both irradiated and dark samples was subsequently used to calculate the specific photocatalytic activity (P_{MB}) according to Equation (2).

$$P_{MB} = R_{irr} - R_{dark} \tag{2}$$

Finally, the photonic efficiency (ζ_{MB}) of the samples was determined using Equation (3).

$$\zeta_{MB} = P_{Mb}/E_P \times 100 \quad (3)$$

where E_P is the light radiation intensity (W/m^2).

The test was replicated 3 times to increase the accuracy and reliability of the results.

3. Results and Discussion

3.1. Characterization of TiO_2 Thin Films

The GAXRD patterns of Ag-TiO_2 coatings with varying Ag contents (2.5 - 7.5 mol%) deposited on glazed ceramic tiles are shown in **Figure 1**. The XRD analysis revealed clear diffraction peaks corresponding to the anatase phase (2θ = 25.4˚, 63.7˚, 68.7˚), rutile phase (2θ = 27.4˚, 35.8˚, 43.5˚, 54.4˚, 57.6˚), and brookite phase (2θ = 39.8˚, 40.8˚, 47.6˚, 52.9˚), confirming the presence of these typical TiO_2 polymorphs. In addition, distinct metallic silver (Ag-4H) peaks were observed at 2θ = 42.8˚, 48.3˚, and 54.9˚, even at the lowest Ag content (2.5 mol%), indicating the successful incorporation of silver into the TiO_2 matrix.

Quantitatively, the intensity of the Ag-4H peaks, particularly at 2θ = 54.9˚, increased with Ag content up to 5 mol%, after which a noticeable decrease in intensity was observed at 7.5 mol%. This trend suggests a saturation point or an agglomeration of Ag nanoparticles at higher doping levels. The enhanced Ag peak intensity at 5 mol% aligns with the findings of Cruz *et al.* [19], who reported an increase in Ag-related peaks in Ag/TiO_2 photocatalysts with increasing Ag content (0.05 - 0.2 mol), synthesized via a modified combustion method. This increase in peak intensity at optimal doping concentration (5 mol%) likely corresponds to the formation of stable Ag-TiO_2 phases that contribute to enhanced photocatalytic activity.

However, at 7.5 mol% Ag content, the reduction in Ag-related peak intensity suggests that higher silver concentrations may lead to silver agglomeration or the formation of less active phases, as also reported by Demirci *et al.* [20]. They observed a decrease in the XRD peak intensity of Ag-doped TiO_2 films (0.1% - 0.9% Ag) on silicon substrates, which they attributed to the reduced crystallinity of the films. This decrease in crystallinity may result from the segregation of Ag ions outside the TiO_2 lattice, as indicated by the unchanged diffraction angles and a broader peak width. Such segregation can hinder the formation of a stable TiO_2-Ag solid solution, potentially reducing photocatalytic efficiency.

The presence of both anatase and rutile phases in all samples suggests mixed-phase TiO_2 coatings, which is consistent with previous studies indicating that the anatase phase is generally more photocatalytically active than rutile, though the latter can provide structural stability [21]. The formation of the brookite phase in the coatings is less common but can contribute to photocatalytic activity by offering additional surface sites for photocatalytic reactions. The coexistence of these phases indicates that the Ag doping might influence the crystallization behavior of TiO_2, leading to a fine balance between phase formation and photocatalytic performance.

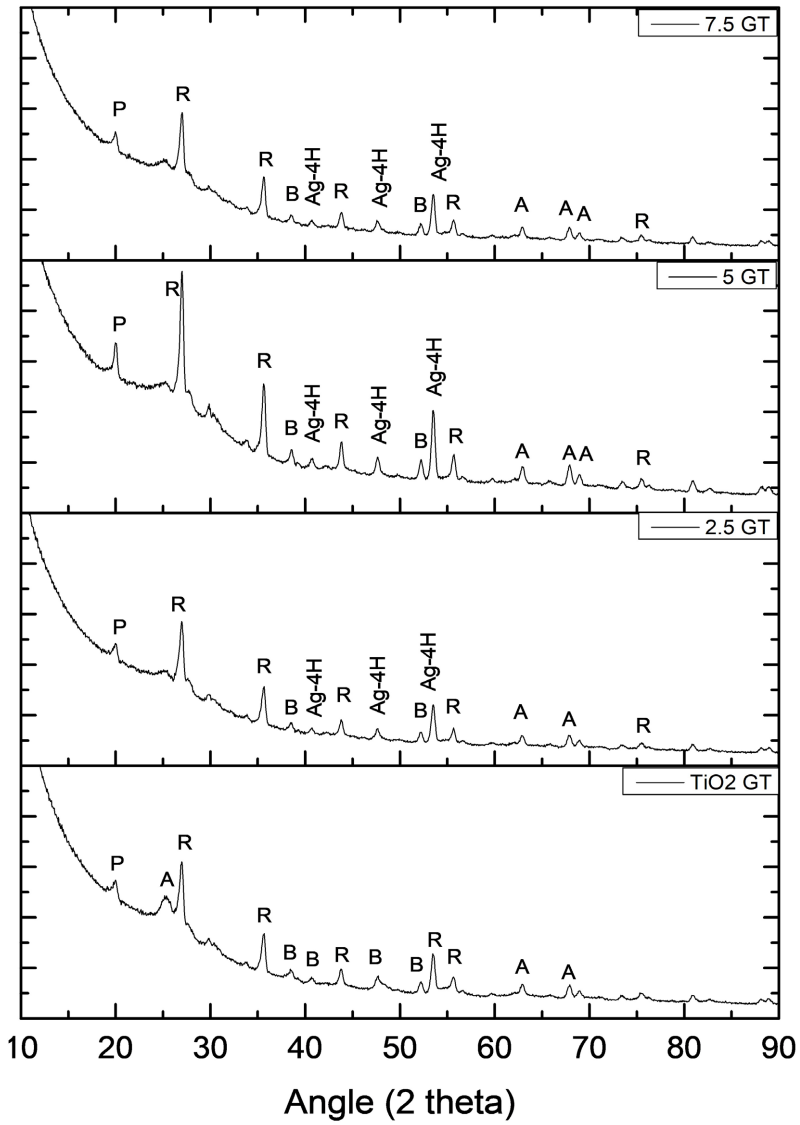


Figure 1. GAXRD pattern of TiO_2 and Ag-TiO_2 coating with varied Ag content deposited on glazed ceramic tiles.

Table 1 summarizes the crystallite sizes of anatase and rutile phases in Ag-TiO_2 coatings as a function of Ag content. Rutile crystallite size remains largely unchanged across all doping levels, indicating minimal influence from Ag incorporation. In contrast, the anatase crystallite size increases from 8.46 nm (0 mol% Ag) to a maximum of 14.5 nm at 5 mol% Ag, then decreases to 10.8 nm at 7.5 mol%. This trend suggests that moderate Ag doping promotes crystallite growth, likely by enhancing nucleation and reducing surface energy, while excess Ag disrupts crystal development, which is consistent with observations by Cruz *et al.* [19].

Figure 2 shows the FWHM values of Ag-TiO_2 coatings on glazed ceramic tiles as a function of Ag content. The FWHM decreases from 0.98˚ at 0 mol% Ag to 0.78˚ at 2.5 mol% Ag, indicating improved crystallinity. However, at 5 mol% Ag, the FWHM increases back to 0.98˚, and then decreases again to 0.78˚ at 7.5 mol%

Ag. These fluctuations suggest that moderate Ag doping enhances crystallinity, while higher concentrations may introduce structural disruptions.

Table 1. Crystallite size of TiO_2 and Ag-TiO_2 coating deposited on glazed ceramic tile.

Photocatalyst sample	Crystallite size (nm)	
	Anatase	Rutile
TiO_2	8.6	28.9
2.5 mol% Ag-TiO_2	10.8	21.7
5 mol% Ag-TiO_2	14.5	21.7
7.5 mol% Ag-TiO_2	10.8	24.7

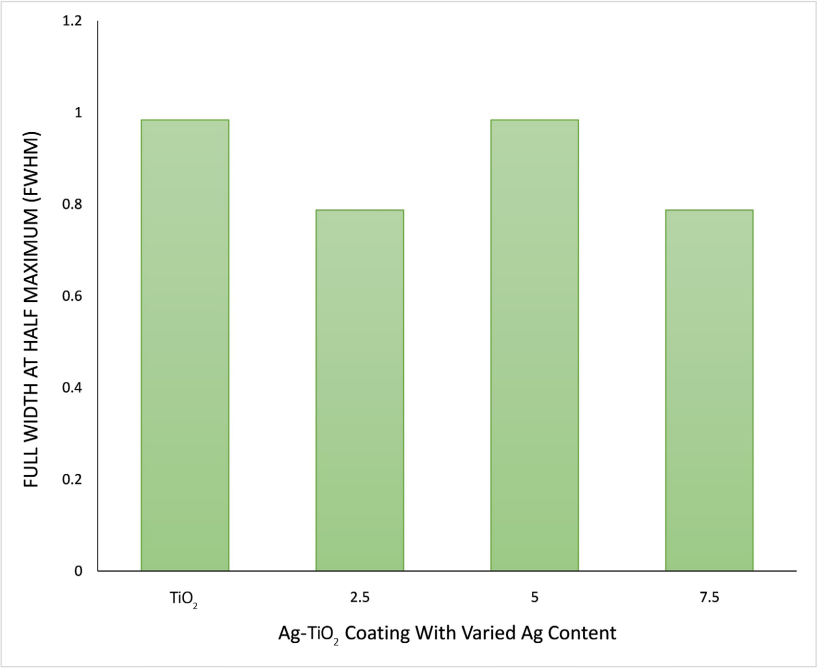


Figure 2. FWHM of Ag-TiO_2 coated on glazed ceramic tiles.

At 2.5 mol% Ag, the reduction in FWHM indicates better crystallite growth, likely due to Ag facilitating anatase formation [22]. The increase at 5 mol% Ag may be due to excess Ag introducing defects or lattice strain, which hinders crystallite order. The subsequent decrease at 7.5 mol% Ag could reflect partial reorganization of the crystal structure, though not a return to optimal order. This behavior is consistent with findings by Cruz *et al.* [19], who demonstrated that while moderate Ag doping improves crystallinity, higher doping levels lead to lattice defects and disorder. These results are further supported by previous studies on doped TiO_2 systems, which have shown that dopant-induced crystallinity enhancement is typically limited by the concentration threshold, beyond which disorder dominates [23]. The observed trends in FWHM and crystallite size highlight the

importance of controlled Ag incorporation in optimizing the structural properties of Ag-TiO_2 coatings for various applications.

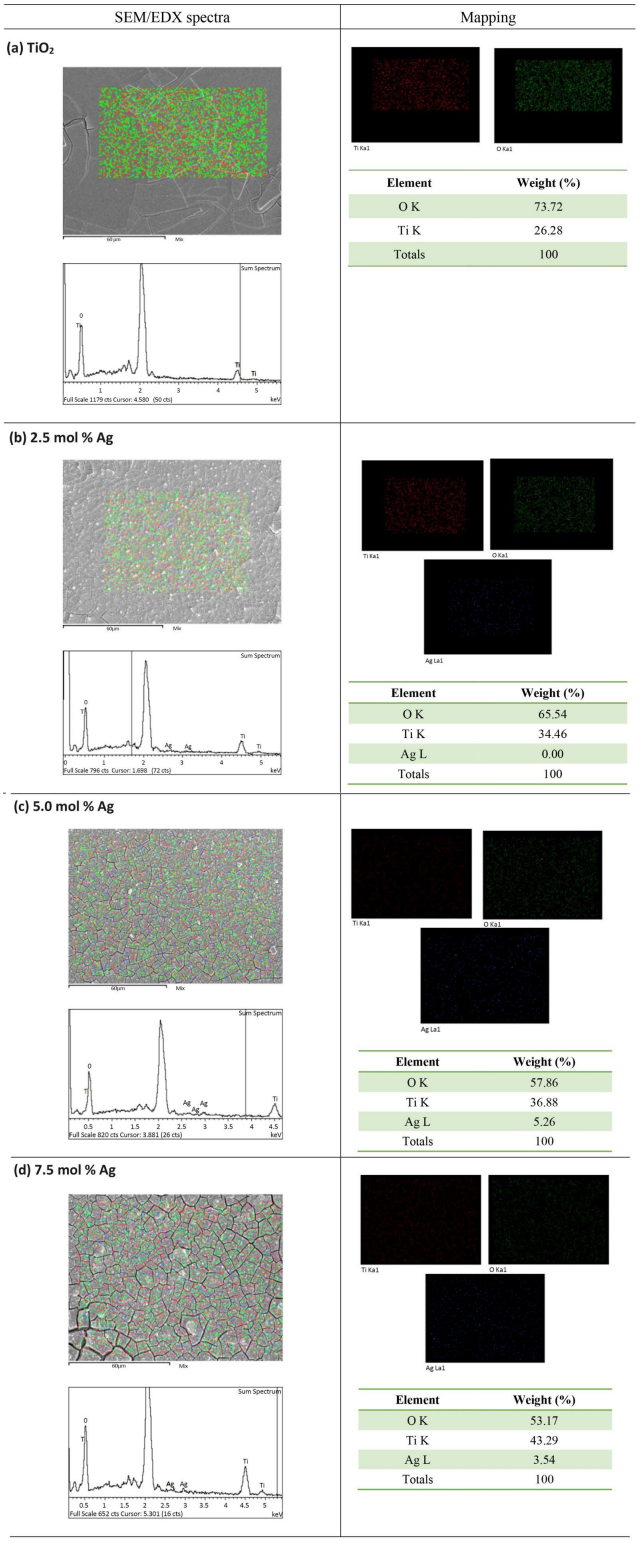


Figure 3. SEM and elemental mapping of Ti, oxygen and Ag for (a) TiO_2 (0% Ag); (b) 2.5 mol% Ag; (c) 5.0 mol% Ag; (d) 7.5 mol% Ag of Ag-TiO_2 coating deposited on glazed tile.

Figure 3 summarizes the EDX and mapping analysis of Ag-TiO_2 coatings with varying Ag content (2.5, 5, and 7.5 mol%) on glazed ceramic tiles. The EDX spectrum confirms the presence of titanium (Ti), oxygen (O), and silver (Ag) on the coated surface, indicating successful Ag-TiO_2 composite formation. Peaks at 0.5 keV, 4.5 keV, and 4.9 keV correspond to Ti, while the oxygen element is observed at 0.6 keV. Weak peaks at 3 keV and 2.7 keV indicate the presence of silver, with a strong peak at 2 keV attributed to the gold coating used in sample preparation.

It was found that the Ag weight percentages were 0%, 5.26%, and 3.54% for the 2.5, 5, and 7.5 mol% Ag-TiO_2 coatings, respectively. The Ag content at 2.5 mol% was below the detection limit of the EDX analysis, consistent with the sensitivity of the technique at low concentrations. This result is in line with previous studies indicating that higher Ag concentrations (5 - 7.5 mol%) are more easily detected, with silver incorporation being most effective at intermediate doping levels [24].

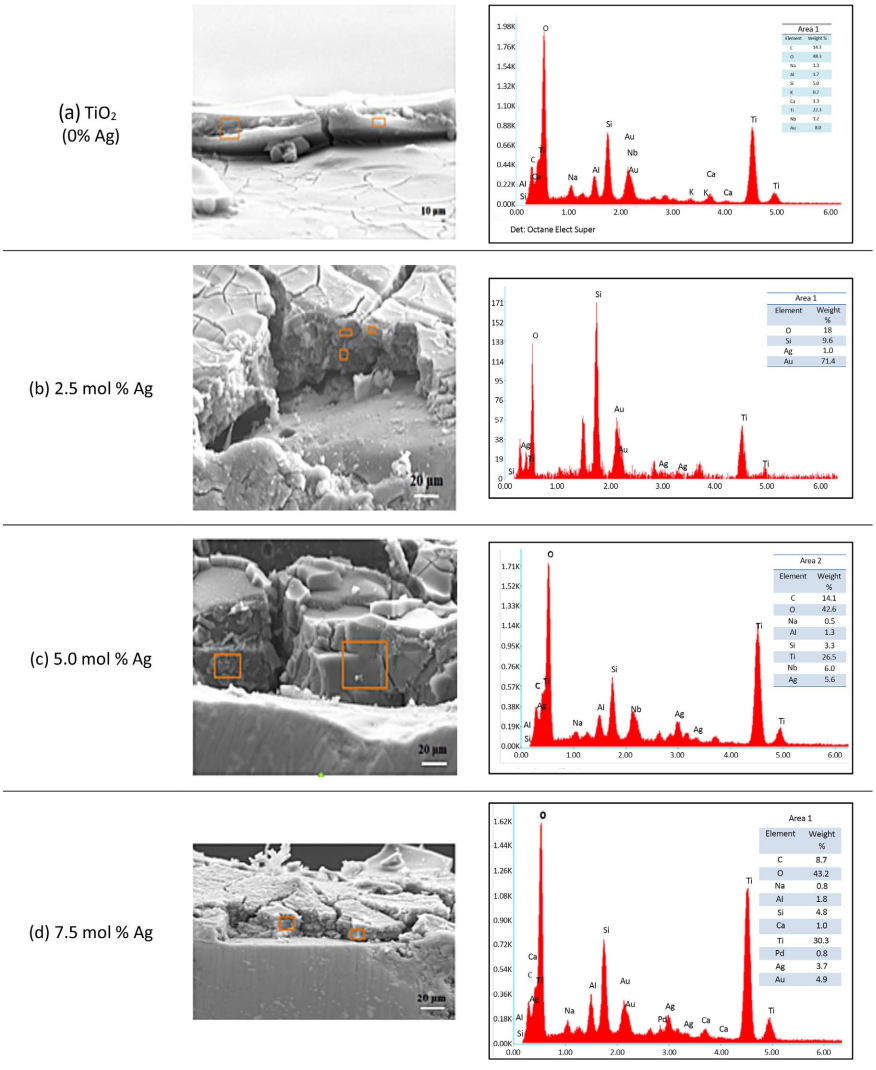


Figure 4. SEM cross section of (a) TiO_2; (0% Ag); (b) 2.5 mol% Ag; (c) 5.0 mol% Ag; (d) 7.5 mol% Ag of Ag-TiO_2 coating deposited on glazed tile.

SEM/EDX mapping further reveals that Ag particles are uniformly distributed on the surface of the coatings. The Ti, O, and Ag particles are found to overlap, suggesting interaction between silver and the TiO_2 matrix, which supports the findings of Mazheika *et al.* (2011) that silver clusters interact with TiO_2(100) surfaces by overlapping with Ti d orbitals, facilitating Ag-TiO_2 composite formation [25]. These results demonstrate the successful integration of silver into TiO_2 coatings and its uniform distribution, which may influence the coatings' photocatalytic or structural properties.

Cross-sectional analysis (**Figure 4**) confirmed the formation of a distinct coating layer on all glazed ceramic tiles. The TiO_2-only coating exhibited a thin layer (1.07 ± 0.73 μm), suggesting limited material deposition and potentially lower photocatalytic activity, as reported in previous studies [26]. Incorporation of Ag at 2.5, 5.0, and 7.5 mol% increased the coating thickness to 9.12 ± 3.04 μm, 14.30 ± 1.20 μm, and 5.26 ± 1.58 μm, respectively. The maximum thickness at 5.0 mol% Ag indicates enhanced film growth and dispersion of Ag within the TiO_2 matrix, which may improve surface reactivity and antibacterial performance [27]. The subsequent decrease at 7.5 mol% is likely due to particle aggregation and increased surface roughness, consistent with findings by Liaqat *et al.* [28], where excessive Ag content led to agglomeration and structural defects. Fractures and uneven coating layers were also observed, attributed to both agglomeration and the multilayer dip-coating process, where drying between successive layers introduces variability [29]. These observations highlight the critical need to optimize Ag concentration and deposition parameters to ensure uniform, crack-free coatings with consistent functional properties.

3.2. Photocatalytic Degradation of Methylene Blue under Visible Light Irradiation

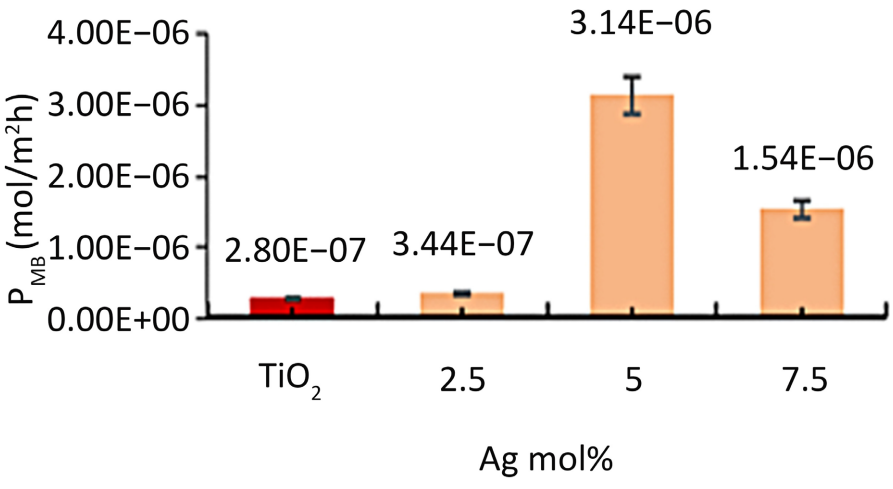


Figure 5. Photocatalytic activity of Ag-TiO_2 coating on glazed tile exposed under visible light irradiation.

The photocatalytic activity and photonic efficiency of Ag-doped TiO_2 coatings on

glazed ceramic tiles under visible light irradiation are shown in Figure 5 and Figure 6. The 5 mol% Ag formulation showed the highest observed photocatalytic performance among the tested coatings, reaching a maximum degradation rate of 3.14×10^{-6} mol/m^2·h and a photonic efficiency of 7.89×10^{-7}%. Silver-related enhancement of visible-light absorption and charge separation may contribute; however, coating thickness and morphology may also affect the comparison. Specifically, Ag acts as an electron trap, reducing electron-hole recombination and enabling more efficient photocatalysis through localized surface plasmon resonance and the formation of mid-gap states [30] [31]. Nevertheless, the maximum activity observed at 5 mol% Ag could be also related due to the increase in crystallite size, a higher coating thickness and its surface morphology. Here, the thickness increase from 1.07 μm for undoped TiO_2 to 14.30 μm at 5 mol% Ag may contribute to the higher observed activity through differences in catalyst loading and morphology.

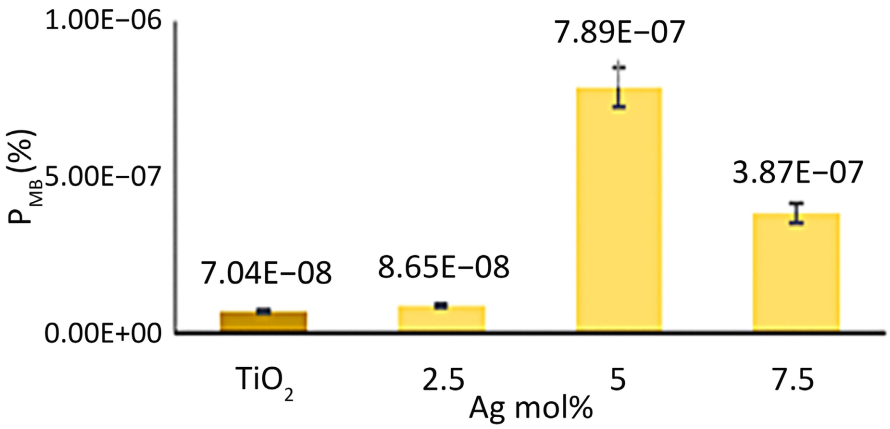


Figure 6. Photonic efficiency of Ag-TiO_2 coating on glazed tile exposed under visible light irradiation.

4. Conclusion

This study successfully enhanced the photocatalytic activity of TiO_2 coatings on glazed ceramic tiles through silver (Ag) doping, addressing the limitations of pure TiO_2 under visible light. Among the tested formulations, 5 mol% Ag showed the highest observed photocatalytic performance under the tested UV and visible-light conditions. Because the anatase crystallite size increased to 14.5 nm at this composition, the result cannot be attributed to reduced crystallite size; coating thickness and morphology may also contribute. These findings demonstrate that Ag-doped TiO_2 coatings can be effectively activated by visible light, offering a practical solution for self-cleaning ceramic surfaces. Elemental mapping showed Ti, O, and Ag across the coated surfaces; however, the observed fractures and uneven layers indicate morphological nonuniformity, and aggregation cannot be ruled out. This work presents an original approach to optimizing Ag content for visible-light photocatalysis, with potential applications in environmental and an-

tibacterial fields. Future studies should focus on evaluating the long-term stability and practical performance of these coatings under real-world conditions, paving the way for their broader application in industrial and environmental technologies.

Acknowledgements

The authors would like to acknowledge the Faculty of Industrial and Manufacturing Technology and Engineering, Universiti Teknikal Malaysia Melaka (UTeM) for the support of this research.

Author Contributions

Nurhafizah Zaharuddin: Investigation, Data Curation, Formal Analysis, and Writing (Original Draft Preparation). Zulkifli Mohd. Rosli: Methodology, Validation, Writing (Review & Editing). Jariah Mohamad Juoi: Conceptualization, Supervision, Validation, Writing (Review & Editing). Thangaraj Joseph Sahaya Anand: Validation and Writing (Review). All authors contributed to the interpretation of the results, critically reviewed the manuscript, approved the final version of the manuscript, and agreed to be accountable for all aspects of the work.

Conflicts of Interest

The authors declare no conflicts of interest regarding the publication of this paper.

References

[1] Kim, J., Kim, U., Han, K. and Choi, J. (2022) Antibacterial Persistence of Hydrophobically Glazed Ceramic Tiles. *Journal of the Korean Ceramic Society*, **59**, 920-928. https://doi.org/10.1007/s43207-022-00216-x

[2] La Torre, V., Rambaldi, E., Masi, G., Nici, S., Ghezzi, D., Cappelletti, M., *et al.* (2021) Validation of Antibacterial Systems for Sustainable Ceramic Tiles. *Coatings*, **11**, Article No. 1409. https://doi.org/10.3390/coatings11111409

[3] Abdellah, M.H., Nosier, S.A., El-Shazly, A.H. and Mubarak, A.A. (2018) Photocatalytic Decolorization of Methylene Blue Using TiO_2/UV System Enhanced by Air Sparging. *Alexandria Engineering Journal*, **57**, 3727-3735. https://doi.org/10.1016/j.aej.2018.07.018

[4] Canbaz, G.T., Çakmak, N.K., Eroğlu, A. and Açıkel, Ü. (2019) Removal of Acid Orange 74 from Wastewater with TiO_2 Nanoparticle. *International Advanced Researches and Engineering Journal*, **3**, 75-80. https://izlik.org/JA75ES82LE

[5] Lu, Z., Zhou, H.F., Liao, J.J., Yang, Y.Y., Wang, K., Che, L.M., *et al.* (2019) A Facile Dopamine-Assisted Method for the Preparation of Antibacterial Surfaces Based on Ag/TiO_2 Nanoparticles. *Applied Surface Science*, **481**, 1270-1276. https://doi.org/10.1016/j.apsusc.2019.03.174

[6] Kamrosni, A.R., Dewi Suryani, C.H., Azliza, A., Mustafa, A.B.A.M., Anuar, M.S.M.A., Norsuria, M., *et al.* (2022) Microstructural Studies of Ag/TiO_2 Thin Film; Effect of Annealing Temperature. *Archives of Metallurgy and Materials*, **67**, 241-245. https://doi.org/10.24425/amm.2022.137496

[7] Chakhtouna, H., Benzeid, H., Zari, N., Qaiss, A.e.k. and Bouhfid, R. (2021) Recent Progress on Ag/TiO_2 Photocatalysts: Photocatalytic and Bactericidal Behaviors. *En-*

vironmental Science and Pollution Research, **28**, 44638-44666. https://doi.org/10.1007/s11356-021-14996-y

[8] Grabowska, E., Zaleska, A., Sorgues, S., Kunst, M., Etcheberry, A., Colbeau-Justin, C., *et al.* (2013) Modification of Titanium(IV) Dioxide with Small Silver Nanoparticles: Application in Photocatalysis. *The Journal of Physical Chemistry C*, **117**, 1955-1962. https://doi.org/10.1021/jp3112183

[9] Mahdieh, Z.M., Shekarriz, S. and Taromi, F.A. (2021) The Effect of Silver Concentration on Ag-TiO_2 Nanoparticles Coated Polyester/Cellulose Fabric by *in Situ* and *Ex Situ* Photo-Reduction Method—A Comparative Study. *Fibers and Polymers*, **22**, 87-96. https://doi.org/10.1007/s12221-021-9049-6

[10] Meydanju, N., Pirsa, S. and Farzi, J. (2022) Biodegradable Film Based on Lemon Peel Powder Containing Xanthan Gum and TiO_2-Ag Nanoparticles: Investigation of Physicochemical and Antibacterial Properties. *Polymer Testing*, **106**, Article ID: 107445. https://doi.org/10.1016/j.polymertesting.2021.107445

[11] Hidayat, A., Taufiq, A., Supardi, Z.A.I., Jayadininggar, S.M., Sa'adah, U., Astarini, N.A., *et al.* (2021) Synthesis and Characterization of TiO_2/ZnO-Ag@TiO_2 Nanocomposite and Their Performance as Photoanode of Organic Dye-Sensitized Solar Cell. *Materials Today: Proceedings*, **44**, 3395-3399. https://doi.org/10.1016/j.matpr.2020.11.862

[12] Kamat, P.V. (2002) Photophysical, Photochemical and Photocatalytic Aspects of Metal Nanoparticles. *The Journal of Physical Chemistry B*, **106**, 7729-7744. https://doi.org/10.1021/jp0209289

[13] Nguyen, H., Park, J., Kang, S. and Kim, M. (2015) Surface Plasmon Resonance: A Versatile Technique for Biosensor Applications. *Sensors*, **15**, 10481-10510. https://doi.org/10.3390/s150510481

[14] Zheng, X., Zhang, D., Gao, Y., Wu, Y., Liu, Q. and Zhu, X. (2019) Synthesis and Characterization of Cubic Ag/TiO_2 Nanocomposites for the Photocatalytic Degradation of Methyl Orange in Aqueous Solutions. *Inorganic Chemistry Communications*, **110**, Article ID: 107589. https://doi.org/10.1016/j.inoche.2019.107589

[15] Pohan, L.A.G., Kambiré, O., Nasir, M. and Ouattara, L. (2020) Photocatalytic and Antimicrobial Properties of $AgTiO_2$: Clay Nanocomposite Prepared with Clay Different Ratios. *Modern Research in Catalysis*, **9**, 47-61. https://doi.org/10.4236/mrc.2020.94004

[16] Onna, D., Fuentes, K.M., Spedalieri, C., Perullini, M., Marchi, M.C., Alvarez, F., *et al.* (2018) Wettability, Photoactivity, and Antimicrobial Activity of Glazed Ceramic Tiles Coated with Titania Films Containing Tungsten. *ACS Omega*, **3**, 17629-17636. https://doi.org/10.1021/acsomega.8b03339

[17] Ashraf, M.A., Liu, Z., Peng, W., Jermsittiparsert, K., Hosseinzadeh, G. and Hosseinzadeh, R. (2020) Combination of Sonochemical and Freeze-Drying Methods for Synthesis of Graphene/Ag-Doped TiO_2 Nanocomposite: A Strategy to Boost the Photocatalytic Performance via Well Distribution of Nanoparticles between Graphene Sheets. *Ceramics International*, **46**, 7446-7452. https://doi.org/10.1016/j.ceramint.2019.11.241

[18] Abbad, S., Guergouri, K., Gazaout, S., Djebabra, S., Zertal, A., Barille, R., *et al.* (2020) Effect of Silver Doping on the Photocatalytic Activity of TiO_2 Nanopowders Synthesized by the Sol-Gel Route. *Journal of Environmental Chemical Engineering*, **8**, Article ID: 103718. https://doi.org/10.1016/j.jece.2020.103718

[19] Cruz, D., Ortiz-Oliveros, H.B., Flores-Espinosa, R.M., Ávila Pérez, P., Ruiz-López, I.I. and Quiroz-Estrada, K.F. (2022) Synthesis of Ag/TiO_2 Composites by Combustion Modified and Subsequent Use in the Photocatalytic Degradation of Dyes. *Jour-*

nal of King Saud University—Science, **34**, Article ID: 101966. https://doi.org/10.1016/j.jksus.2022.101966

[20] Demirci, S., Dikici, T., Yurddaskal, M., Gultekin, S., Toparli, M. and Celik, E. (2016) Synthesis and Characterization of Ag Doped TiO_2 Heterojunction Films and Their Photocatalytic Performances. *Applied Surface Science*, **390**, 591-601. https://doi.org/10.1016/j.apsusc.2016.08.145

[21] Jacob, K.A., Peter, P.M., Jose, P.E., Balakrishnan, C.J. and Thomas, V.J. (2022) A Simple Method for the Synthesis of Anatase-Rutile Mixed Phase TiO_2 Using a Convenient Precursor and Higher Visible-Light Photocatalytic Activity of Co-Doped TiO_2. *Materials Today*: *Proceedings*, **49**, 1408-1417. https://doi.org/10.1016/j.matpr.2021.07.104

[22] Li, J., Jin, Z., Zhang, Y., Liu, D., Ma, A., Sun, Y., *et al.* (2022) Ag-Induced Anatase-Rutile TiO_{2-x} Heterojunction Facilitating the Photogenerated Carrier Separation in Visible-Light Irradiation. *Journal of Alloys and Compounds*, **909**, Article ID: 164815. https://doi.org/10.1016/j.jallcom.2022.164815

[23] Bakar, S.A. and Ribeiro, C. (2016) Nitrogen-Doped Titanium Dioxide: An Overview of Material Design and Dimensionality Effect over Modern Applications. *Journal of Photochemistry and Photobiology C*: *Photochemistry Reviews*, **27**, 1-29. https://doi.org/10.1016/j.jphotochemrev.2016.05.001

[24] Zaharuddin, N., Mohamad Juoi, J., Mohd Rosli, Z., Johari, N.D. and Moriga, T. (2024) Effect of Silver Doping on the Microstructure and Photocatalytic Performance of Ag-TiO_2 Coatings on Unglazed Ceramic. *Journal of Advanced Research in Micro and Nano Engineering*, **25**, 14-26. https://doi.org/10.37934/armne.25.1.1426

[25] Mazheika, A.S., Bredow, T., Matulis, V.E. and Ivashkevich, O.A. (2011) Theoretical Study of Adsorption of Ag Clusters on the Anatase TiO_2(100) Surface. *The Journal of Physical Chemistry C*, **115**, 17368-17377. https://doi.org/10.1021/jp200575u

[26] Tian, S., Feng, Y., Zheng, Z. and He, Z. (2023) TiO_2-Based Photocatalytic Coatings on Glass Substrates for Environmental Applications. *Coatings*, **13**, Article No. 1472. https://doi.org/10.3390/coatings13081472

[27] Zarzzeka, C., Goldoni, J., de Paula de Oliveira, J.d.R., Lenzi, G.G., Bagatini, M.D. and Colpini, L.M.S. (2024) Photocatalytic Action of Ag/TiO_2 Nanoparticles to Emerging Pollutants Degradation: A Comprehensive Review. *Sustainable Chemistry for the Environment*, **8**, Article ID: 100177. https://doi.org/10.1016/j.scenv.2024.100177

[28] Liaqat, M.A., Hussain, Z., Khan, Z., Akram, M.A. and Shuja, A. (2020) Effects of Ag Doping on Compact TiO_2 Thin Films Synthesized via One-Step Sol-Gel Route and Deposited by Spin Coating Technique. *Journal of Materials Science*: *Materials in Electronics*, **31**, 7172-7181. https://doi.org/10.1007/s10854-020-03288-9

[29] Mathew Simon, S., George, G., M S, S., V P, P., Anna Jose, T., Vasudevan, P., *et al.* (2021) Recent Advancements in Multifunctional Applications of Sol-Gel Derived Polymer Incorporated TiO_2-ZrO_2 Composite Coatings: A Comprehensive Review. *Applied Surface Science Advances*, **6**, Article ID: 100173. https://doi.org/10.1016/j.apsadv.2021.100173

[30] Kien, K.D.T., Nhi, N.V.U., Minh, H.N. and Minh, D.Q. (2022) Optical Properties of the Bi_2O_3-B_2O_3-ZnO Glass System Combined with TiO_2 or Ag/TiO_2. *Journal of Ceramic Processing Research*, **23**, 350-355.

[31] Komaraiah, D., Radha, E., Sivakumar, J., Ramana Reddy, M.V. and Sayanna, R. (2020) Photoluminescence and Photocatalytic Activity of Spin Coated Ag^+ Doped Anatase TiO_2 Thin Films. *Optical Materials*, **108**, Article ID: 110401. https://doi.org/10.1016/j.optmat.2020.110401